Quantum Electronics **52** (5) 465–468 (2022)

INTERACTION OF LASER RADIATION WITH MATTER. LASER PLASMA https://doi.org/10.1070/QEL18044

Superluminescence in the phonon wing of the photoluminescence spectrum of NV centres in diamond optically pumped at $\lambda = 532$ nm

E.I. Lipatov, D.E. Genin, M.A. Shulepov, E.N. Tel'minov, A.D. Savvin, A.P. Eliseev, V.G. Vins

Abstract. **Superluminescence of NV centres with a band peaking at $\lambda = 718$ nm in the phonon wing of the photoluminescence spectrum of a high-pressure high-temperature (HPHT) diamond sample under pulsed optical excitation at $\lambda = 532$ nm with an intensity of 2–46 MW cm^{-2} is demonstrated. Superluminescence is observed in the diamond crystal region containing 6 ppm NV centres and 150 ppm substituent nitrogen; it is absent in the crystal part with a lower nitrogen content. Superluminescence pulses are observed on the leading edge of the optical excitation pulse at $\lambda = 532$ nm and have an FWHM value of 4 ns. The enhancement of the photoluminescence of NV centres is suggested to be due to the total internal reflection in the diamond plate (waveguide effect).**

Keywords: *diamond, laser, superluminescence, photoluminescence, NV centre, optical pumping.*

1. Introduction

Diamond containing impurity–defect centres photoactive in the visible spectral range is a promising base for quantum information technologies: quantum calculations and quantum cryptography [1]. Here, promising candidates are nitrogen–vacancy centres in the negative charge state (NV centres) and vacancy–IV-group element centres (SiV, GeV, SnV, and PbV centres) [2]. NV centres are of particular interest for quantum optical technologies in view of the high nitrogen solubility in the diamond lattice [3], long coherence time of quantum states of NV centres at room temperature [4], and strong electron–phonon interaction [5].

The potential possibility of implementing multiqubit calculations on NV centres in diamond with controlled optical and microwave radiation suggests realisation of optical integrated circuits on the diamond surface, which contain visible light sources and NV centres acting as qubits.

To date, laser radiation sources based on NV centres have not been developed because of the poor quality of synthetic diamond samples, nonuniform distribution of impurities in them, and the existence of NV centres in three charge states (–, 0, +) [6]. Since the vibronic bands of point centres in solids are characterised by discrepancy between absorption and luminescence profiles, visible light in the range of 500–635 nm must be used for optical pumping of NV centres. Amplification and lasing should be expected in the phonon wing of the luminescence spectrum, i.e., in the vicinity of $\lambda = 720$ nm [7].

We reported previously [8] that amplification and lasing were observed for diamond sample C29 in the phonon wing of the luminescence spectrum of NV centres in a wide band with a maximum at $\lambda = 719$ nm. In this study we report observation of superluminescence for diamond sample C31 in the phonon wing of the luminescence spectrum of NV centre in a wide band peaking at $\lambda = 718$ nm under pulsed optical pumping at $\lambda = 532$ nm.

2. Experimental

A schematic of the experiment is presented in Fig. 1. Pulsed radiation at $\lambda = 532$ nm of the second harmonic of a LQ215*LG103T Nd:YAG laser (SOLAR Laser Systems) was used to excite photoluminescence (PL) in diamond sample C31 with sizes of $4.44 \times 4.41 \times 0.25$ mm. The energy of radiation pulse at the laser system output was 80 mJ at an FWHM of ~10 ns. The laser beam (pump) intensity in the range of 0.1–50 MW cm^{-2} was varied using light filters of the HC1, HC2 and HC6 types (*2*). The radiation was focused on the large faces of diamond sample C31 into a spot 0.5×3.0 mm in size by two cylindrical lenses *3* with a focal length of 15 cm in one out of three characteristic regions with different impurity–defect compositions, which are indicated in the image of sample C31 in Fig. 2c. Photoluminescence was recorded through the small faces of a sample with sizes of 4.44×0.25 or 4.41×0.25 mm at an angle of 10–30° with respect to the large-face plane. The small sample faces were not polished. The luminescence light was directed through optical fibre *5* to AvaSpec-2048-2 spectrometer (Avantes) *6*, the data from which, with allowance for the spectral sensitivity and fibre transmittance, were converted into a digital file and then presented in the graphical format using the OriginPro 9 software. All measurements were performed under normal conditions at room illumination in the end of January and beginning of February, 2021, at the Tomsk State University.

E.I. Lipatov, D.E. Genin, M.A. Shulepov Laboratory of Quantum Information Technologies, National Research Tomsk State University, prosp. Lenina 36, 634050 Tomsk, Russia; Institute of High Current Electronics, Siberian Branch, Russian Academy of Sciences, prosp. Akademicheskii 2/3, 634055 Tomsk, Russia; e-mail: lipatov@loi.hcei.tsc.ru;
E.N. Tel'minov, A.D. Savvin Laboratory of Quantum Information Technologies, National Research Tomsk State University, prosp. Lenina 36, 634050 Tomsk, Russia;
A.P. Eliseev Institute of Geology and Mineralogy, Siberian Branch, Russian Academy of Sciences, prosp. Akad. Koptyuga 3, 630090 Novosibirsk, Russia;
V.G. Vins Velman Ltd., ul. Russkaya 43, 630058 Novosibirsk, Russia

Received 30 September 2021; revision received 14 January 2022
Kvantovaya Elektronika **52** (5) 465–468 (2022)
Translated by Yu.P. Sin'kov

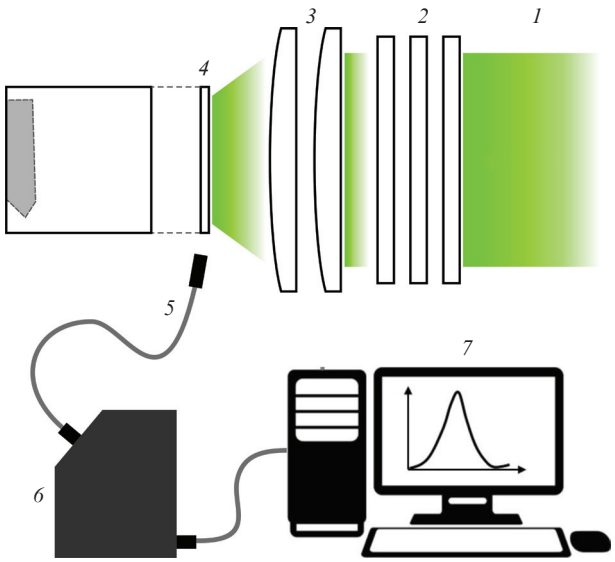

Figure 1. (Colour online) Schematic of the experiment: (*1*) pulsed laser radiation at $\lambda = 532$ nm; (*2*) light filters; (*3*) cylindrical lenses; (*4*) diamond sample; (*5*) optical fibre; (*6*) spectrometer; (*7*) computer.

The diamond sample was cut from a crystal synthesised under HPHT conditions. The distribution of substituent nitrogen in it was initially nonuniform (1–150 ppm); i.e., sample C31 exhibited the so-called sectorality: nonuniform impurity distribution in dependence of the growth sectors. After polishing the large faces, sample C31 was subjected to radiative-thermal treatment in two stages: irradiation by 3-MeV electrons to a surface dose of 10^{19} cm^{-2} with subsequent annealing in vacuum at 1000 °C for 2 h.

Table 1 contains the concentrations of substituent nitrogen (N_S) and NV centres in the negative charge state in each of three characteristic regions of the diamond samples produced by Velman Ltd. (Novosibirsk, Russia), according to the manufacturer's data. There is no information about the concentration of NV centres in the neutral charge state.

Table 1. Concentrations of substituent nitrogen NS and nitrogen–vacancy complexes in the negative charge state NV– in three regions of diamond sample C31. The concentrations are given in ppm (1 ppm ≈ 1.763 × 1018 cm–3).

Region 2	Concentration N_S /ppm	Concentration NV^- /ppm
1	150	6.1
2	5	1.2
3	130	2.9

The optical absorption spectra of diamond sample C31 in the range of 200–900 nm and IR absorption spectra in the range of 700–2300 cm^{-1} are shown in Fig. 2. The absorption spectra were calculated from the transmission spectra according to the standard technique [9]. The transmission spectra in the range from 200 to 900 nm were measured using a Shimadzu UV-2501 RS spectrometer with a spectral resolution of 1 nm. The measurements in the IR range with a spectral resolution of 2 cm^{-1} were performed using a Bruker Vertex 70 FTIR spectrometer jointly with a Hyperion 2000 microscope.

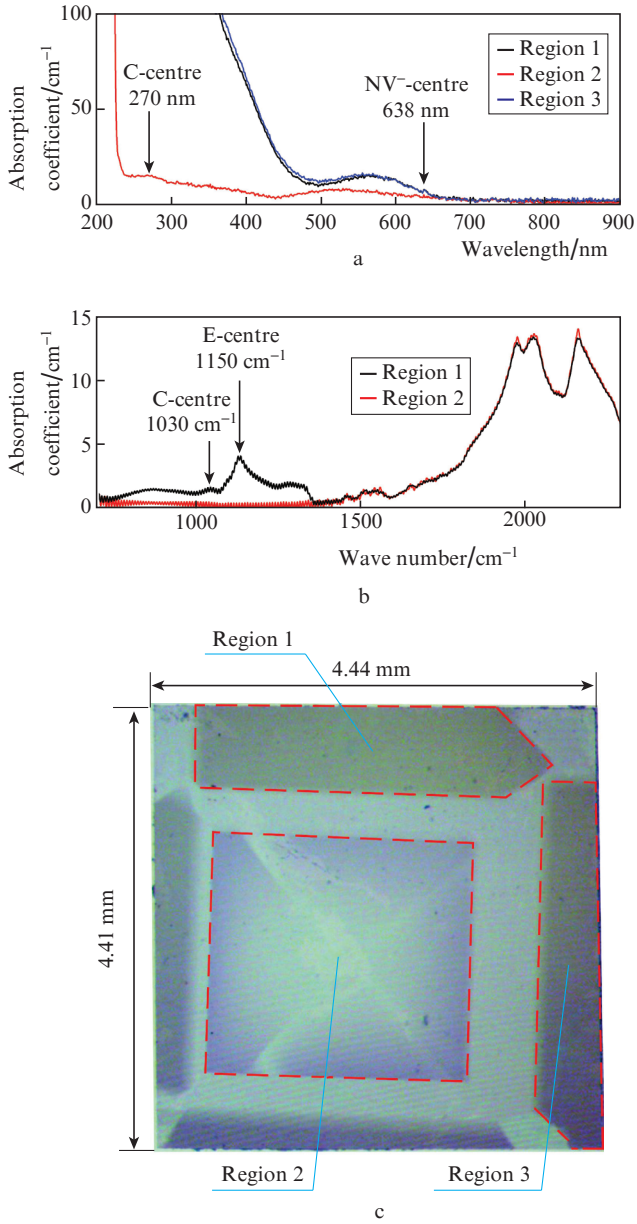

Figure 2. (Colour online) Absorption spectra of diamond sample C31 in the (a) optical and (b) IR ranges and (c) a photograph of diamond sample C31 with the aforementioned characteristic regions.

Spectral region 2 (Fig. 2a) demonstrates a fundamental absorption edge at $\lambda = 225$ nm; substituent-nitrogen band at $\lambda = 270$ nm (C centre); and a wide band from 440 to 640 nm, formed by phonon wings in the absorption spectrum of NV^0 and NV centres. Regions 1 and 3 are characterised by almost identical optical properties in the measured ranges, strong absorption in the UV spectral region, a weak zero-phonon line (ZPL) of NV centres at $\lambda = 638$ nm, and a phonon wing of NV centres in the range of 500–640 nm.

The IR spectrum (Fig. 2b) of region 2 does not contain any substituent-nitrogen band. At the same time, the spectra of regions 1 and 3 contain absorption bands at frequencies of 1030 and 1150 cm^{-1} (C and E centres, respectively), which are due to the substituent nitrogen, and a wide band peaking at 350–900 cm^{-1}, which is assigned to the radiative effect of electrons [5]. No other spectral features were observed.

3. Results and discussion

The photoluminescence spectra of diamond sample C31 under optical pumping at $\lambda = 532$ nm are shown in Fig. 3. The spectra are normalised to the intensity corresponding to the maximum of unperturbed phonon wing of the NV-centre spectrum at 680–690 nm and to the ZPL intensity for NV^0 centres at $\lambda = 575$ nm. In addition, the luminescence spectra of NV^0 and NV centres reported in [10] are shown in Fig. 3 for comparison.

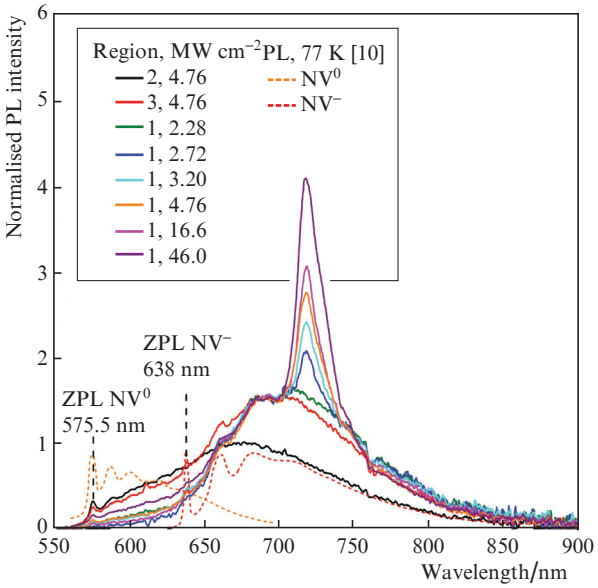

Figure 3. (Colour online) Photoluminescence spectra of diamond sample at optical pump intensities from 2.28 to 46 MW cm^{-2} (indicated in the figure) at $\lambda = 532$ nm, obtained for three characteristic regions of the sample (dashed curves are the luminescence spectra of NV^0 and NV centres from [10]).

The spectra of region 2 are characterised by the presence of ZPL of NV^0 centres and phonon wing of NV^0 centres, the absence of ZPL of NV centres, and the presence of a weak phonon wing of NV centres at all pump intensities in the range of 0.1–50 MW cm^{-2}.

The spectra of region 3 exhibit the presence of both the vibronic system of NV^0 centres and the vibronic system of NV centres at all pump intensities.

The vibronic system of NV^0 centres in the spectrum of region 1 is highly weak, but the vibronic system of NV centres is fairly intense, with a distinguishable ZPL at $\lambda = 638$ nm.

With an increase in the pump intensity above ~2.0 MW cm^{-2}, an additional band started manifesting itself in the wavelength range of 700–760 nm in the PL spectrum of region 1 of sample C31; at a pump intensity above 2.5 MW cm^{-2} this band was observed in the form of a strong peak with a maximum at $\lambda = 718.3$ nm. The FWHM value for this peak increased from 13 to 19 nm with an increase in the pump intensity from 2.7 to 46 MW cm^{-2}. The nature of this peak can be explained in terms of enhanced spontaneous emission, i.e. superluminescence, as shown in Fig. 4. Here, pump radiation (*1*) penetrated a diamond sample to excite NV centres (*2*), randomly oriented along four directions. The NV-centre luminescence with wavelengths of 700–760 nm, which was directed to large sample faces at an angle smaller than the total internal reflection angle θ_C, was minimally amplified; it left the sample through large faces (*3*). The PL directed at maximum angles to the sample large faces was amplified much more strongly; it left the sample through small faces (*4*). The PL that obeyed the total internal reflection conditions was enhanced maximally due to the waveguide effect and maximal path length in the sample. This radiation was recorded in the some range of optimal angles to large faces of the sample (*5*). Currently, we cannot explain the maximum enhancement of photoluminescence at $\lambda = 718$ nm; additional studies should be performed.

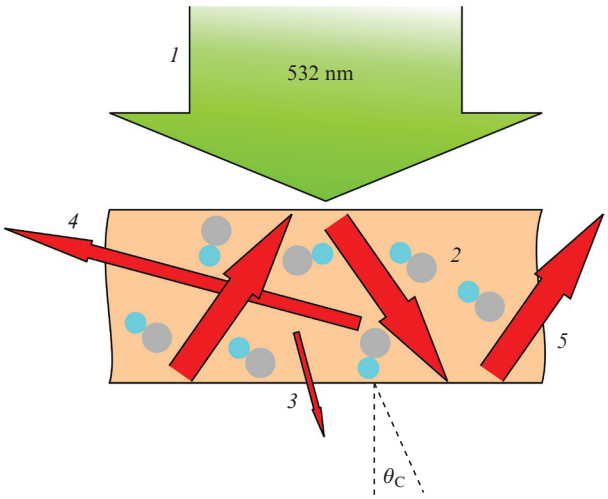

Figure 4. (Colour online) Schematic of the occurrence of superluminescence band peaking at $\lambda = 718$ nm in the photoluminescence spectrum of diamond sample under optical pumping at $\lambda = 532$ nm.

The dependence of PL intensity in the spectral maximum, I_{PL}, on the pump intensity I_{532} obeys the logarithmic law: $I_{PL} = \text{Const1} + \text{Const2} \times \ln I_{532}$ (Fig. 5). In the absence of superluminescence band in the spectrum (at pump intensities below 2 MW cm^{-2}), the slope of the dependences in the same for all three regions (empty red, blue, and green symbols in Fig. 5). The transition region (filled red circles in Fig. 5) corresponds to the pump intensity range of 2–3 MW cm^{-2}. At pump intensities above 3 MW cm^{-2} the slope of the dependence for region 1 sharply increases, and then, in the intensity range from 5 to 10 MW cm^{-2}, this dependence tends to saturation.

A DET10A/M photodiode (Thorlab) and TDS-2022B oscilloscope (Tektronix) were used to record photoluminescence pulses in region 1 of sample C31 for different pump intensities at $\lambda = 532$ nm. Oscillograms of PL and pump radiation pulses are shown in Fig. 6. The pump pulse width at $\lambda = 532$ nm turned out to be ~10 ns at half maximum and about 30 ns at the base level.

It can be seen in Fig. 6 that, at a pump intensity of 0.32 MW cm^{-2}, the shape of the PL pulse repeated on the whole the shape of the pump pulse, but the luminescence pulse maximum was observed approximately 1 ns after the pump pulse maximum, and the trailing edge of the PL pulse was delayed with respect to the pump pulse.

At a pump intensity of 3.2 MW cm^{-2} the luminescence pulse maximum shifted in time and was ahead of the pump pulse maximum by 1.5 ns. The trailing edge of the PL pulse was also delayed relative to the pump pulse.

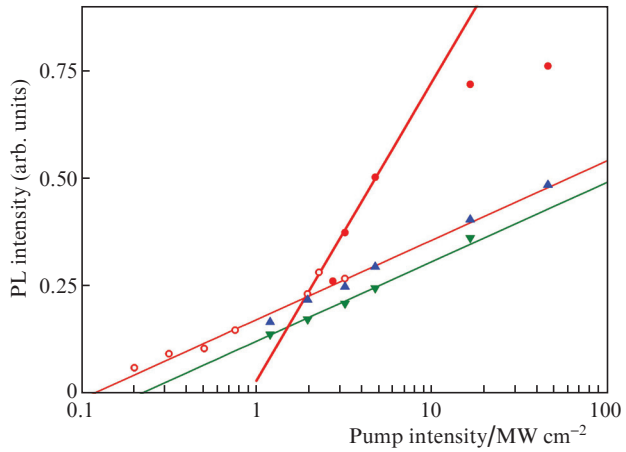

Figure 5. (Colour online) Dependences of the PL intensity on the pump intensity at λ = 532 nm for three regions of diamond sample C31 (red, blue, and green points correspond to regions 1, 2, and 3, respectively); solid lines are approximations of the dependences by logarithmic functions).

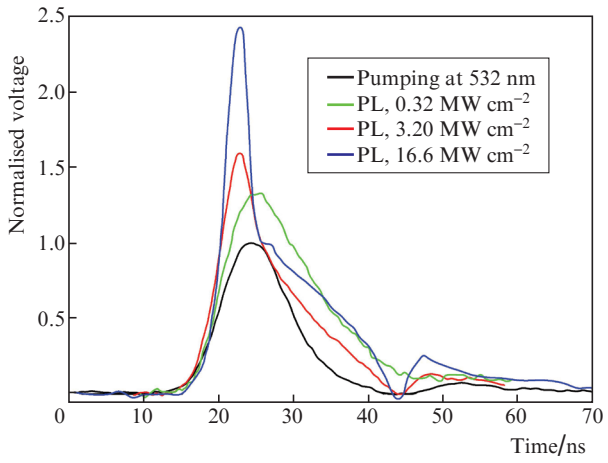

Figure 6. (Colour online) Oscillograms of the pump pulse at λ = 532 nm and PL pulses in region 1 of sample C31 at pump intensities of 0.32, 3.2, and 16.6 MW cm^{-2}.

At a pump intensity of 16.6 MW cm^{-2}, the PL pulse maximum was also ahead of the pump pulse maximum by 1.5 ns. The luminescence pulse was composed of at least two pulses (more pronounced than at a pump intensity of 3.2 MW cm^{-2}): the first dominant pulse with an FWHM of ~4 ns and the second, less intense by a factor of 2.5 and delayed with respect to the pump pulse.

4. Conclusions

Our investigations demonstrated superluminescence of NV centres in the negative charge state for HPHT diamond sample C31, in the crystal region containing 6 ppm NV centres and 150 ppm substituent nitrogen. Superluminescence was observed under pulsed optical excitation at λ = 532 nm with an intensity of more than 2 MW cm^{-2} at the leading edge of the pump pulse in the phonon wing of the photoluminescence spectrum of NV centres with a maximum at λ = 718 nm. Enhancement of the spontaneous emission of NV centres occurred due to the increase in the optical path of PL luminescence as a result of the total internal reflection in the diamond plate (waveguide effect).

In the future we have to determine the influence of the impurity–defect composition of samples in wide ranges of concentrations and optical pump wavelengths on the superluminescence, calculate and measure the gain and loss in the samples, observe lasing in the presence of feedback (cavity), explain the nature of the enhancement in the phonon wing of photoluminescence spectrum of NV centres, and verify the presence of PL enhancement for other photoactive centres in diamond.

Acknowledgements. This work was performed within a State Assignment of the Ministry of Science and Higher Education of the Russian Federation (Project No. 0721-2020-0048). We are grateful to A.G. Korotaev, Dean of the Faculty of Radiophysics, founder of the Quantum Centre of the National Research Tomsk State University, for the administrative support of the study.

References

1. Suter D., Jelezko F. *Prog. Nucl. Magn. Reson. Spectrosc.*, **98–99**, 50 (2017). DOI: 10.1016/j.pnmrs.2016.12.001.
2. Ekimov E.A., Kondrin M.V., Krivobok V.S., et al. *Diam. Relat. Mater.*, **93**, 75 (2019). DOI: 10.1016/j.diamond.2019.01.029.
3. Khomich A.A., Kudryavtsev O.S., Bolshakov A.P., et al. *J. Appl. Spectrosc.*, **82** (2), 242 (2015). DOI: 10.1007/s10812-015-0092-1.
4. Stanwix P.L., Pham L.M., Maze J.R., et al. *Phys. Rev. B.*, **82**, 201201 (2010). DOI: 10.1103/PhysRevB.82.201201.
5. Zaitsev A.M. *Optical Properties of Diamond: A Data Handbook* (Springer-Verlag, 2001).
6. Lobaev M.A., Radishev D.B., Bogdanov S.A., et al. *Phys. Status Solidi*, **14** (11), 2000347 (2020). DOI: 10.1002/pssr.202000347.
7. Nair S.R., Rogers L.J., Vidal X., et al. *Nanophotonics*, **9** (15), 4505 (2020). DOI: 10.1515/nanoph-2020-0305.
8. Savvin A., Dormidonov A., Smetanina E., et al. *Nat. Commun.*, **12**, 7118 (2021). DOI: 10.1038/s41467-021-27470-7.
9. Lipatov E.I., Lisitsyn V.M., Oleshko V.I., et al., in *Cathodoluminescence*. Ed. by N. Yamamoto (InTech, 2012). DOI: 10.5772/32321.
10. Lu H.-C., Peng Y.-C., Chou S.-L., et al. *Angew. Chem. Int. Ed.*, **56** (46), 14469 (2017). DOI: 10.1002/anie.201707389.